

# Unprecedented Approach for Using Misoprostol Alongside Low-Dose Gamma Radiation to Alleviate Paraquat-Induced Pulmonary Injury in Rats

Dose-Response:  
An International Journal  
Vol. 23(1): 1–12  
© The Author(s) 2025  
Article reuse guidelines:  
[sagepub.com/journals-permissions](https://sagepub.com/journals-permissions)  
DOI: 10.1177/15593258251326707  
[journals.sagepub.com/home/dos](https://journals.sagepub.com/home/dos)



Ahmed H. Youssef<sup>1</sup> , Heba H. Mansour<sup>1</sup> , Wafaa Gh. Shousha<sup>2</sup>, Shereen M. Galal<sup>1</sup>, and Sara M. Abdo<sup>2</sup>

## Abstract

**Background:** Abrupt inflammation and alveolar epithelial membrane damage, which may cause the alveolar membrane's malfunction, are related to acute lung injury (ALI). This could eventually lead to pulmonary fibrosis. While lung injury can happen in many ways, the current study will concentrate on the changes in lung pathology mediated by paraquat (PQ). Paraquat, a widely used herbicide, targets lung toxicity through inflammation and oxidative stress, which significantly contribute to lung damage.

**Objective:** The current research was to ascertain whether low-dose gamma radiation (R) and misoprostol (MP) could lessen the lung inflammatory cascade started by PQ injection in rats.

**Methods:** The ALI model was induced by I.P. injection of PQ (20 mg/kg once), and then treatment was done by MP and/or R for 14 days, and finally, the biochemical and histological parameters were measured in the lung tissues.

**Results:** Our data suggest that PQ can promote ALI through TGF- $\beta$ /smad, Notch, NF- $\kappa$ B, and ET-1 signaling pathways, resulting in EMT. These suggestions were supported by increased levels of TGF- $\beta$ , inflammatory cytokines,  $\alpha$ -SMA, NF- $\kappa$ B, ET-1, CTGF protein, and LPA, whereas PPAR- $\gamma$  decreased. The aforementioned results have been confirmed by lung histopathology.

**Conclusion:** We suggest that the pulmonary inflammatory cascade was hindered and all the previously described gauges improved with R and/or MP therapy.

## Keywords

paraquat, acute lung injury, gamma-irradiation, misoprostol, epithelial mesenchymal transition

Received: 5 August 2024; accepted: 23 January 2025

## Introduction

The hallmarks of acute respiratory distress syndrome (ARDS) and acute lung injury (ALI) are edema (swelling of the lungs), inflammation (both local and systemic), and abnormalities in the alveoli, all of which contribute to hypoxemia and eventual lung failure.<sup>1</sup> The development of ALI is attributed to the inflammatory processes that result in increased accessibility of the capillary arteries in the lungs and extensive damage affecting the alveoli.<sup>2,3</sup> As a result of lung injury, a change occurs in macrophages, causing them

<sup>1</sup> Health Radiation Research Department, National Centre for Radiation Research & Technology, Egyptian Atomic Energy Authority, Cairo, Egypt

<sup>2</sup> Department of Chemistry, Faculty of Science, Helwan University, Cairo, Egypt

### Corresponding Author:

Ahmed H. Youssef, Health Radiation Research Department, National Centre for Radiation Research & Technology, Egyptian Atomic Energy Authority, Cairo 11787, Egypt.  
Email: [ahagaga113@gmail.com](mailto:ahagaga113@gmail.com)



Creative Commons Non Commercial CC BY-NC: This article is distributed under the terms of the Creative Commons Attribution-NonCommercial 4.0 License (<https://creativecommons.org/licenses/by-nc/4.0/>) which permits non-commercial use, reproduction and distribution of the work without further permission provided the original work is attributed as specified on the SAGE and Open Access pages (<https://us.sagepub.com/en-us/nam/open-access-at-sage>).

to adopt M1 phenotypes that promote inflammation and start to secrete proinflammatory cytokines (interleukin-1 (IL-1), tumor necrosis factor- $\alpha$  (TNF- $\alpha$ ), interleukin-6 (IL-6)) and chemokines (IL-8, CCL7, CCL2), which cause raised chemotaxis and ongoing enhancement of alveolar spaces by monocytes and neutrophils.<sup>4</sup> Neutrophils, in response, produce many mediators of inflammation, including reactive oxygen species (ROS) and proteinases, which cause damage to surfactant, basal membranes, and the epithelial-endothelial barrier.<sup>5</sup> While undergoing ALI development, the destruction of alveolar epithelial type II cells (AEC II) causes a substantial decline in surfactant production. Consequently, the alveolar disruption causes a cascade of proteins to enter the alveolar space, besides the subsequent spreading of pulmonary edema,<sup>6</sup> the formation of hyaline membranes during the exudative phase, and the deposition of extracellular matrix (ECM) during the proliferative phase.<sup>7,8</sup> In some cases, inflammation transforms from acute into chronic, which may result in fibrosis progression. Myofibroblasts, which are a distinct type of fibroblasts with contractile abilities, have a vital role in both wound healing and the pulmonary fibrosis progress.<sup>9</sup> During the process of lung tissue restoration, myofibroblasts engage in active synthesis of ECM components. In a healthy organism, these myofibroblasts are naturally discarded during apoptosis once an adequate quantity of ECM has been produced. However, in the context of chronic inflammation, myofibroblasts persist and avoid apoptosis, leading to the development of aberrant wound healing, extravagant ECM production, and ultimately, pulmonary fibrosis. The conversion of fibroblasts into myofibroblasts is typically coordinated by the presence of transforming growth factor beta (TGF- $\beta$ 1) and mechanical stress.<sup>10</sup> There are a great number of causative factors of ALI and ARDS, counting bacterial and viral pneumonia, continuous mechanical ventilation, chemicals, electronic cigarettes, acute brain injury, sepsis, acute pancreatitis, and others.<sup>11</sup>

Paraquat (1,1'-dimethyl-4,4'-bipyridinium dichloride, PQ) is a commonly used defoliant known for its extreme toxicity to people, resulting in significant fatality rates. This is due to its tremendous toxicity and the absence of an effective rescue approach.<sup>12</sup> PQ primarily accumulates within the lung tissues, especially in type I and type II pneumocytes as well as Clara cells, at levels approximately 6 to 10 times higher than those found in plasma.<sup>13</sup> PQ poisoning leads to a two-phase lung pathology characterized by destructive and proliferative stages. During the destructive phase, there is swelling and fragmentation of the alveolar epithelium, along with alveolar edema and acute inflammation. In the proliferative phase, fibroblasts infiltrate the alveolar space, resulting in diffuse intra-alveolar fibrosis.<sup>14</sup> PQ induces lung damage and fibrosis via various molecular pathways, including matrix metalloproteinase-9 (MMP-9), peroxisome proliferator-activated receptor-gamma (PPAR- $\gamma$ ), caspase cleavage, nuclear factor kappa-light-chain-enhancer of activated B cells (NF- $\kappa$ B), jun N-terminal kinase/p38 mitogen-activated protein kinase (JNK/p38 MAPK), nuclear factor erythroid 2-related factor 2/NADPH oxidase4 (Nrf2/Nox4)

redox balance, and transforming growth factor-beta/small mothers against decapentaplegic3 (TGF- $\beta$ 1/Smad3) signaling pathways.<sup>15,16</sup> Epithelial mesenchymal transition (EMT) is also one of the central factors of PQ poisoning in which alveolar epithelial cells in the fibrotic areas show the mesenchymal marker alpha smooth muscle actin ( $\alpha$ -SMA), leading to a decrease in the functionality of the alveolar epithelium and a rise in the dysfunction of epithelial-mesenchymal cells.<sup>17</sup> NF- $\kappa$ B, a crucial element of EMT, facilitates the secretion of numerous inflammation-related molecules, including TNF- $\alpha$ , IL-1 $\beta$ , and TGF- $\beta$ . The EMT is brought through the TGF- $\beta$ /smad signaling cascade.<sup>18</sup>

The treatment of PQ poisoning faces numerous challenges, and there is a deficit of universally accepted procedures for managing patients poisoned by PQ. Presently, available therapies for PQ-induced lung injury, which may lead to fibrotic stages, are designed based on inhibiting the inflammatory cascade that triggers the initial damage, including anti-inflammatory medications such as glucocorticoids, as well as immunosuppressive and cytotoxic agents like azathioprine and cyclophosphamide.<sup>19</sup>

Prostaglandin E1 (PGE1) is a member of a group of naturally occurring acidic lipids that possess pulmonary and systemic vasodilator actions, along with anti-inflammatory effects. These medications are considered the established medical treatment for managing arterial pulmonary hypertension.<sup>20</sup> Previous research has demonstrated that administering a low dose of PGE1 can decrease the production of IL-6, enhance oxygenation, and reduce the duration of systemic inflammatory response syndrome.<sup>21</sup> Misoprostol (MP), which is a structural analogue of naturally occurring PGE1, exhibits decreased side effects related to prostaglandins, such as vomiting and diarrhea, and also shows reduced adverse impacts on the circulatory system. It's an FDA-approved medication, prescribed with a recommended dose of 200  $\mu$ g taken orally 4 times a day for preventing or treating Non-Steroidal Anti-Inflammatory Drugs (NSAID)-induced gastric ulcers in high-risk patients. In various diseases or experimental contexts not involving the liver, misoprostol has been documented to lower the secreted inflammatory promoters (TNF- $\alpha$ , IL-6, and IL-8) while increasing IL-10 levels.<sup>22</sup>

Research has been conducted to discover effective therapies for lung injury, including the assessment of low-dose radiation (R). This is based on the logic that R possesses anti-inflammatory and immune-regulating actions, which could potentially neutralize the pro-inflammatory condition seen.<sup>23,24</sup> Cytokines released by macrophages, other immune cells, endothelial cells (EC), and fibroblasts rule the sequence of pulmonary fibrosis. Low-dose radiation could control the cytokine production through its anti-inflammatory activity and accordingly avert the harm brought to lung tissue leading to ALI/ARDS.<sup>25,26</sup>

Hence, the current investigation was conducted to ascertain the prophylactic and curative efficacy of MP (PGE1 analog) and/or R against PQ-induced lung damage in rats.

## Materials and Methods

### Animals

Forty-nine Sprague-Dawley rats, weighing about 0.12–0.15 kg, were obtained from the animal house of Nile Co for the Pharmaceuticals and Chemical Industries. Upon arrival at the animal house of the National Centre for Radiation Research and Technology (NCRRT), Egyptian Atomic Energy Authority, Cairo, Egypt, the animals were housed in controlled environmental circumstances, where they were given a week to acclimate before the start of the experiment. They were kept in conventional cages with regulated temperature and a 12-hour light/dark cycle. The animals had unrestricted access to food and water.

The Research Ethics Committee at NCRRT gave their approval to all experiments, and they were all conducted in accordance with the 2012 CIOMS and ICLAS international guiding principles for biomedical research involving animals, which follow the 3Rs principle of animal experimentation: replace, reduce, refine. The approval number is 53A/23, dated on December 28, 2023.

### Chemicals

PQ was got from Sigma-Aldrich Co (USA) and dissolved in 0.9% NaCl to be prepared for the study. MP was obtained from Sigma Pharmaceutical Industries and was prepared in normal saline.

### $\gamma$ -irradiation

Whole body gamma irradiation was carried out using a Caesium gamma cell provided by the NCRRT at Cairo, Egypt. The type of source used was Caesium-137 (Gamma Cell-40). Animals were irradiated with a total dose of 1 Gray (0.5 Gy once weekly for 2 weeks) delivered at a dose rate of 0.05 Gy/sec.

### Experimental Design

A lung damage model was created in male albino rats by administering PQ (20 mg/kg) intraperitoneally (IP).<sup>27</sup> The power analysis conducted using G\*Power 3.1.9.4 software from Heinrich-Heine Dusseldorf University determined that a total of 49 samples divided into 7 groups should be included in this investigation. The desired test power is set at 85%, with an effect size of 0.65 and a margin of error of 0.05.

The rats were divided into 7 groups (7 rats each) as follows: **Group 1 (control)**, rats were injected with a single dose of saline through I.P. route, and then 1 day after saline injection, the rats received oral saline for 2 weeks. **Group 2 (PQ)**, rats were administered a single I.P. injection of PQ at a dose of 20 mg/kg. **Group 3 (MP)**, rats were received oral MP (200  $\mu$ g/kg/day) for 2 weeks.<sup>28</sup> **Group 4 (R)**, entire bodies of rats were exposed to a dose of 1 Gy of  $\gamma$ -irradiation (0.5 Gy

once weekly for 2 weeks).<sup>29</sup> **Group 5 (PQ + MP)**, rats were administered a single I.P. injection of PQ at a dose of 20 mg/kg, and then, 1 day after PQ injection, rats received oral MP (200  $\mu$ g/kg/day) for 2 weeks. **Group 6 (PQ + R)**, rats were administered a single I.P. injection of PQ at a dose of 20 mg/kg, and then, 1 day after PQ injection rats were exposed to whole-body  $\gamma$ -irradiation of 1 Gy (0.5 Gy once weekly for 2 weeks). **Group 7 (PQ + MP + R)** rats were administered a single I.P. injection of PQ at a dose of 20 mg/kg, and then, 1 day after PQ injection, rats were exposed to whole-body  $\gamma$ -irradiation of 1 Gy (0.5 Gy once weekly for 2 weeks) combined with oral MP (200  $\mu$ g/kg/day) for 2 weeks.

### Preparation of Lung Tissue Homogenate

After the study completion (after 15 days), all rats were anaesthetized with urethane (Sigma Aldrich Co, USA; 1.5 g/kg, I.P.) and sacrificed. The lung tissues were extracted, and one lobe of the lung was promptly immersed in a 10% neutral buffered formalin solution for subsequent histological evaluations. A tissue homogenate was prepared using the other lobe of the lung in a potassium phosphate buffer with a pH of 7.4. The homogenates that were obtained were divided into smaller portions and promptly stored at a temperature of  $-80^{\circ}\text{C}$  for the purpose of conducting Western blot analysis and measuring various oxidative and antioxidant parameters.

### Biochemical Parameters Measurements

*Assessment of Some Proinflammatory Cytokines, NF- $\kappa$ B, Nrf2, and Lysophosphatidic Acid (LPA) in Lung Tissue Using ELISA.* The microplates provided were coated with  $1^{\text{st}}$  antibodies for LPA, Nrf2, IL-6, TNF- $\alpha$ , IL-1 $\beta$  and NF- $\kappa$ B. Standards or samples were added to the appropriate microplate wells with a biotin-conjugated antibody specific to each of them. Subsequently, Horseradish peroxidase (HRP) coupled with avidin was introduced into every well of the microplate and allowed to incubate. Upon addition of the 3, 3', 5, 5'-tetramethylbenzidine (TMB) substrate solution, a noticeable alteration in color occurred. The enzyme-substrate reaction was halted by the introduction of a solution of sulphuric acid, and the alteration in color was quantitatively assessed using spectrophotometry at a wavelength of 450 nm. The concentration of each parameter is thereafter determined by matching the optical density of the samples to the standard curve.

### Western Blot Analysis

Endothelin-1 (ET-1),  $\alpha$ -SMA, TGF- $\beta$ , connective tissue growth factor (CTGF), and PPAR- $\gamma$  were identified in the lung tissue using Western blot analysis. The lung tissue sample was placed in a lysis solution that has protease suppressors and then homogenized. Protein concentrations were measured using the Bradford reagent. Each sample was loaded with an identical volume of 2 $\times$  sample buffer with 20  $\mu$ g protein

concentration. The sample buffer consisted of 4% SDS, 10% 2-mercaptoethanol, 20% glycerol, 0.004% bromophenol blue, and 0.125 M Tris HCl. The pH level was measured and adjusted to 6.8. Samples were stacked onto an SDS-PAGE gel. Later the isolated proteins were allowed to run for 7 min at 25 V to allow protein bands to transfer from the gel to the membrane made of polyvinylidene difluoride. The nonspecific sites were blocked using Tris-buffered saline with Tween 20 (TBST) buffer and 3% bovine serum albumin for 1 h. The blot was then treated overnight at 4°C with ET-1,  $\alpha$ -SMA, TGF- $\beta$ , CTGF, and PPAR- $\gamma$  antibodies.

The blot was rinsed 3-5 times for 5 min with TBST. Goat anti-rabbit conjugated IgG antibodies were utilized to identify antibodies binding. The incubation process involved exposing the blotted target protein to the HRP-conjugated secondary antibody solution for a duration of 1 h at room temperature. The blot was washed 3-5 times for 5 min with TBST. The chemiluminescent substrate was applied to the blot. The chemiluminescent signals were recorded using a camera-based imager that utilizes a charge-coupled device (CCD) technology. The band intensity of the required proteins was measured against the control sample beta actin (a house-keeping protein) using specific software. This was done by protein normalization on the ChemiDoc MP imager.

### Histopathologic Examinations and Lung Injury Scoring

The lung tissue was fixed using a 10% solution of formalin. After fixation, the lung tissues were inserted in paraffin wax and sliced into sections that were 4-6  $\mu$ m thick. These sections were then stained with hematoxylin and eosin (H&E).<sup>30</sup> Slides were inspected under a light magnifying lens. The extent of interstitial inflammation, alveolar wall thickening, peribronchial inflammation, and interstitial edema in each tissue part of the lung was assessed and assigned a score ranging from 0 to 4. The score corresponded to the percentage of the affected area, with 0 indicating no more than 10% impacted, 1 indicating up to 30% affected, 2 indicating up to 50% affected, 3 indicating up to 70% affected, and 4 indicating 70% or more affected.<sup>31</sup>

### Statistical Analysis

Using GraphPad Prism (version 8.0.2) software, one-way analysis of variance (ANOVA) and Tukey's test as a post-ANOVA test were used to analyze the data, which were reported as mean  $\pm$  S.E. *P* value less than or equal to 0.05 was taken as the significance at a minimum level.

## Results

### Proinflammatory Cytokines TNF- $\alpha$ , IL-1 $\beta$ and IL-6

Some features confirmed the occurrence of paraquat lung damage in our study. The paraquat-intoxicated rats showed a significant increase in the levels of some proinflammatory

cytokines, for example, TNF- $\alpha$ , IL-1 $\beta$ , and IL-6, compared with the control group of rats ( $P < 0.0001$ ). Whereas the individual treatment of MP or R in PQ-administered rats significantly decreased TNF- $\alpha$ , IL-1 $\beta$ , and IL-6 ( $P < 0.0001$ ) as compared with the PQ-intoxicated rats. Compared with the PQ group, the levels of TNF- $\alpha$ , IL-1 $\beta$ , and IL-6 in the combination group (PQ + MP + R) were significantly reduced ( $P < 0.001$ ). Additionally, the combination group (PQ + MP + R) also exerted a significant decline in these proinflammatory mediators compared to the (PQ + MP) and (PQ + R) groups ( $P < 0.001$ ). Finally, the MP and R groups didn't induce any alterations in the preceding parameters in comparison with the normal control rats ( $P > 0.05$ ). (Figure 1).

### NF- $\kappa$ B and Nrf2

Figure 2 revealed that PQ significantly ( $P < 0.0001$ ) raised the level of NF- $\kappa$ B and diminished the Nrf2 level in lung tissues in comparison with those in the control group. In contrast, treatment with either MP or R can reverse these changes in the NF- $\kappa$ B and Nrf2 levels significantly ( $P < 0.0001$ ) in the PQ-administered rats. The combination group (PQ + MP + R) decreased the level of NF- $\kappa$ B and increased the Nrf2 levels significantly ( $P < 0.0001$ ) compared to the PQ group with a result better than that seen in the other treated groups. Against the control group, there were non-significant changes in the levels of NF- $\kappa$ B and Nrf2 in the MP and R groups ( $P > 0.05$ ). (Figure 2)

### LPA

Compared to the control group result, the LPA concentration was significantly ( $P < 0.001$ ) increased in damaged lung tissues after PQ injection. Inversely, the PQ-administered rats treated with either MP or R, especially the MP, induced a significant reduction ( $P < 0.0001$ ) in the LPA level compared to the PQ group.

The MP and R administration in the PQ-intoxicated rats also significantly reduced the level of LPA ( $P < 0.0001$ ) compared to both the PQ group and the other treated groups. The MP and R groups induced a non-significant change in the LPA level compared to the control group ( $P > 0.05$ ). (Figure 3)

### Western Plot Results

Results of rat lung tissue showed that in comparison with the control group, the expression of ET-1,  $\alpha$ -SMA, TGF- $\beta$ , and CTGF in the lung tissue increased while PPAR- $\gamma$  decreased in the PQ-intoxicated rats ( $P < 0.0001$ ). Both the PQ + MP and PQ + R groups significantly decreased the levels of protein expression of ET-1,  $\alpha$ -SMA, TGF- $\beta$ , and CTGF, and PPAR- $\gamma$  expression was significantly raised ( $P < 0.0001$ ) compared with the PQ group. When the PQ-intoxicated rats were treated with MP and R, the expression levels of ET-1,  $\alpha$ -SMA, TGF- $\beta$  and CTGF were significantly reduced, and PPAR- $\gamma$  was upregulated



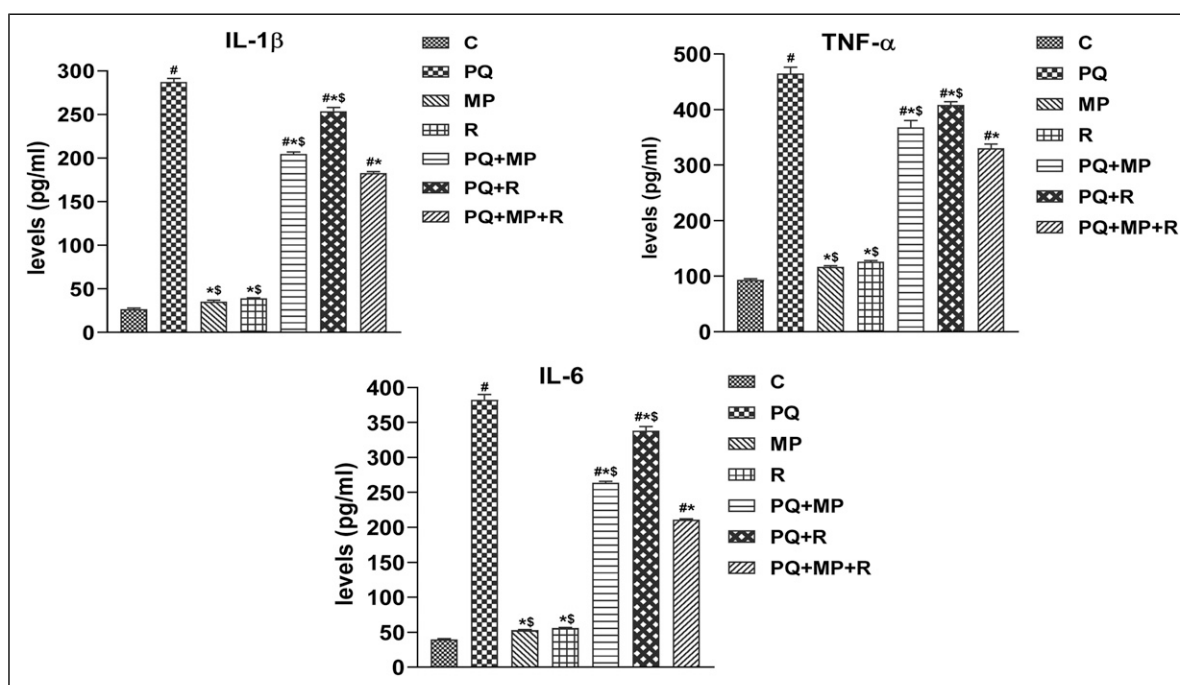


**Figure 1.** Effects of MP and/or R on some proinflammatory cytokines in the PQ-intoxicated rats. The results are expressed as mean  $\pm$  S.E. (n = 7 per group). <sup>#</sup>P  $\leq$  0.05 vs control. <sup>\*</sup>P  $\leq$  0.05 vs PQ-treated group of rats. <sup>\$</sup>P  $\leq$  0.05 vs (PQ + MP + R).

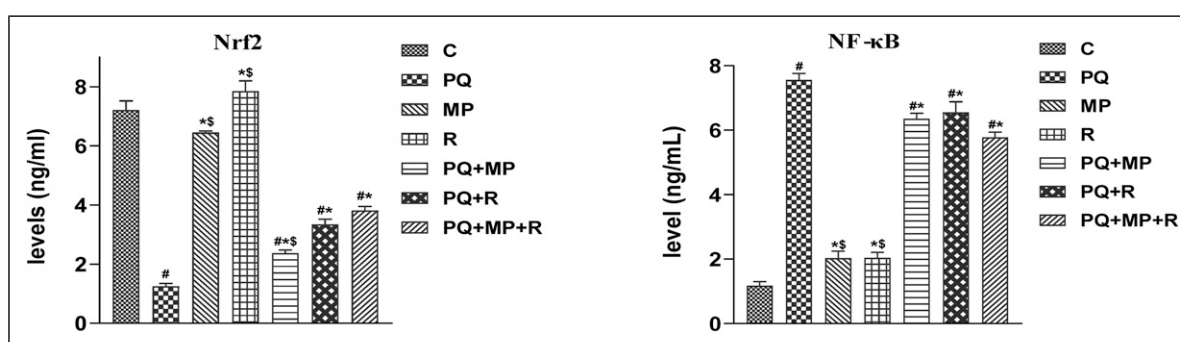


**Figure 2.** Effects of MP and/or R on NF- $\kappa$ B and Nrf2 levels in the PQ-intoxicated rats. The results are expressed as mean  $\pm$  S.E. (n = 7 per group). <sup>#</sup>P  $\leq$  0.05 vs control. <sup>\*</sup>P  $\leq$  0.05 vs PQ-treated group of rats. <sup>\$</sup>P  $\leq$  0.05 vs (PQ + MP + R).

compared to the PQ group, with more effective results than those in the other treated groups ( $P < 0.0001$ ). (Figure 4A and B)

## Histology

Histopathological assessment of paraquat-treated rats showed massive inflammatory cell infiltration of interstitial tissue in-between alveoli, mainly neutrophils, lymphocytes, and macrophages. Perivascular and peribronchial mononuclear cell aggregation. Considerable condensing of the inter-alveolar septa and with full depletion of bronchial goblet cells and exfoliation of epithelial lining were detected. Multifocal collapsed area with alveolar oedema, which appeared as eosinophilic homogenous fluid. Numerous focal

emphysematous regions accompanied by giant alveoli appearances were noticed (Figure 5A and B). Furthermore, PQ significantly increased the lung injury scores (score 4) (Figure 6) in comparison with the control group.

The individual treatment of MP (Figure 5E and F) and R (Figure 5C and D) presented moderate injury, but the severity was significantly alleviated and lung injury score (Figure 6) significantly cut back (score 2) compared with the PQ group.

As shown in Figure 5G and H the combination group, few numbers of cellular aggregation in the interstitium by mononuclear cells, mainly lymphocytes and macrophages, were found in peribronchial and perivascular spaces. Mild thickening of the inter-alveolar septa was identified. Intact alveolar and bronchial epithelial lining were noticed.

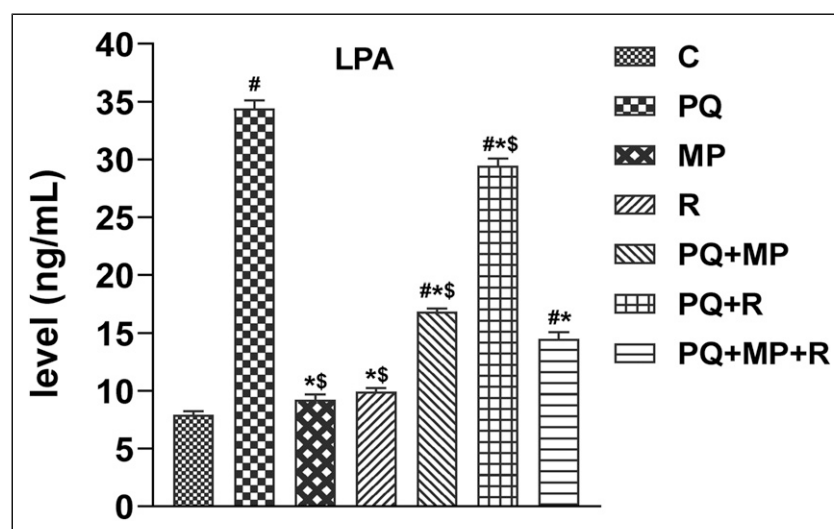


**Figure 3.** Effects of MP and/or R on LPA levels in the PQ-intoxicated rats. The results are expressed as mean  $\pm$  S.E. ( $n = 7$  per group).  $^{#}P \leq 0.05$  vs control.  $^{*}P \leq 0.05$  vs PQ-treated group of rats.  $^{\$}P \leq 0.05$  vs (PQ + MP + R).

Therefore, the lung injury score (Figure 6) significantly lowered (score 1) compared with the PQ group and compared with the PQ + MP and PQ + R groups.

The histopathological examinations for the control (Figure 5I), MP, (Figure 5J) and R (Figure 5K) groups exhibited typical lung structure, with air spaces separated by thin and delicate inter-alveolar septa.

The vasculature appeared normal, with minimal connective tissue surrounding the blood vessels. The bronchioles displayed folded columnar epithelial cells, and the distribution of fibrous tissues was normal.

The alveoli seemed to be expanded with delicate partitions between them, so the lung injury score was 0, like the control group (Figure 6).

## Discussion

The lung tissue is the organ affected mainly during paraquat (PQ) poisoning, which quickly results in the onset of acute lung injury (ALI) and the progression of respiratory failure.<sup>32</sup> In the current work, it was suggested that the transforming growth factor-beta/small mothers against decapentaplegic3 (TGF- $\beta$ /smad), notch pathway, canonical nuclear factor kappa-light-chain-enhancer of activated B cells (NF- $\kappa$ B), and endothelin-1 (ET-1) routes are included in the mechanism of PQ-induced lung tissue injury, and these pathways cooperatively induce epithelial-mesenchymal transition (EMT).

Numerous research findings indicate that TGF- $\beta$ , a versatile cytokine, is pivotal in the fibrosis process by promoting the fibroblasts to be transformed into myofibroblasts and stimulating collagen synthesis.<sup>33</sup> It has been observed that increased TGF- $\beta$  production is linked to PQ-induced lung fibrosis, as well as various chronic inflammatory and fibrotic conditions, in both humans and laboratory animals.<sup>34</sup>

The interaction between TGF- $\beta$  and its receptor initiates the phosphorylation of SMAD2 and SMAD3, leading to their combination with phosphorylated SMAD4 to form a complex.<sup>35</sup> This complex then translocates to the cell nucleus, where it associates with nuclear transcription factors, including connective tissue growth factor (CTGF). It has been noticed that CTGF actively triggers the transcription of genes responsible for some processes like cell proliferation, cell adhesion, cell migration, angiogenesis, and additional physiological processes.<sup>36</sup>

In healthy individuals, CTGF expression is typically minimal; however, during the progression of pulmonary fibrosis, there is a notable rise in CTGF expression, exhibiting a pro-fibrotic impact that leads to the heightened production of TGF- $\beta$ , increased deposition of extracellular matrix (ECM) components, and the suppression of ECM degradation by suppressing metalloproteinases.<sup>37</sup> Based on these discoveries, we noticed in our recent study that the degrees of TGF- $\beta$  and CTGF expression were notably upregulated in PQ-intoxicated rats. These findings confirm the previous reports regarding TGF- $\beta$  and CTGF upregulation.<sup>38</sup> Interestingly, we also found that compared to the low-dose radiation (R) treatment alone, misoprostol (MP) could achieve a more significant suppression of those inflammatory cytokines after PQ injection. Treatment with low-dose radiation (R) reversed the effect of PQ toxicity and led to TGF- $\beta$  and CTGF downregulation.

Interestingly, Rodríguez-Tomás et al<sup>39</sup> (2022) reported a notable decline in inflammation biomarkers like TGF- $\beta$ 1 and C-reactive protein in COVID-19 patients after delivering 0.5 Gy of low-dose radiation singly to the entire lungs. Our study confirmed that administration of MP and/or R attenuates PQ alterations noticeably; this may be because of its anti-inflammatory and antioxidant properties.

The Notch cascade has a marked role in controlling multiple cellular routes like cell differentiation, proliferation, and autophagy. Notch has the ability to trigger EMT in alveolar epithelial

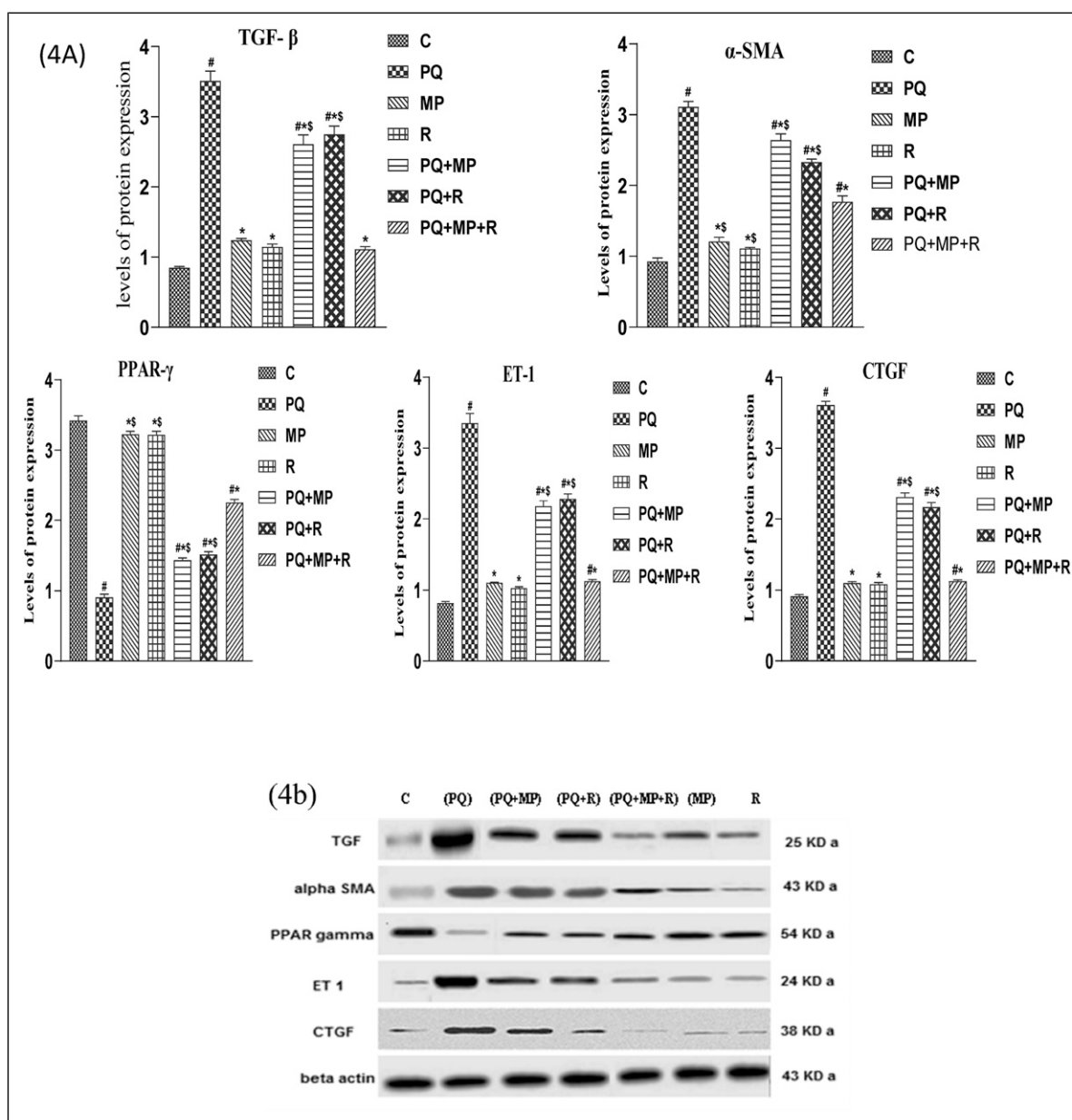


**Figure 4.** Comparison of expression levels of ET-1,  $\alpha$ -SMA, TGF- $\beta$ , CTGF and PPAR- $\gamma$  using western blotting. (A) statistical analysis of protein expression. Data are expressed as mean  $\pm$  S.E. # $P \leq 0.05$  vs control. \* $P \leq 0.05$  vs PQ-treated group of rats. \$ $P \leq 0.05$  vs (PQ + MP + R). (B) Representative graphs of protein expression.

cells by interacting with TGF- $\beta$ , resulting in pulmonary interstitial fibrosis evolution. This condition is distinguished by the appearance of alpha smooth muscle actin ( $\alpha$ -SMA) as a marker.<sup>40</sup> Myofibroblasts that express  $\alpha$ -SMA are actively involved in the synthesis of ECM components. This process leads to the gradual and irreversible disruption of the intact lung architecture, as it gets replaced with connective tissue. Ultimately, this results in a disturbance of gas exchange and leads to pulmonary failure.<sup>41</sup>

So, in the ongoing study, PQ was found to trigger ALI through the raised expression levels of  $\alpha$ -SMA in the PQ group. Other studies also confirmed the involvement of the Notch signal in the

EMT process via the TGF- $\beta$ /Smad3 pathway, and this mechanism potentially plays a role in the transformation of alveolar epithelial cells into myofibroblasts during the advancement of pulmonary fibrosis triggered by PQ poisoning.<sup>42</sup> Misoprostol treatment could significantly decrease the expression levels of  $\alpha$ -SMA and TGF- $\beta$  compared with the PQ group. It is shown that low-dose radiation vs acute inflammatory lung damage lowers the paraquat-induced elevation of  $\alpha$ -SMA levels, referring to its beneficial effects that have also been confirmed by an earlier study by Arenas et al.<sup>43</sup> (2021) that reported the presence of an enhancement in respiratory complications, clinical parameters



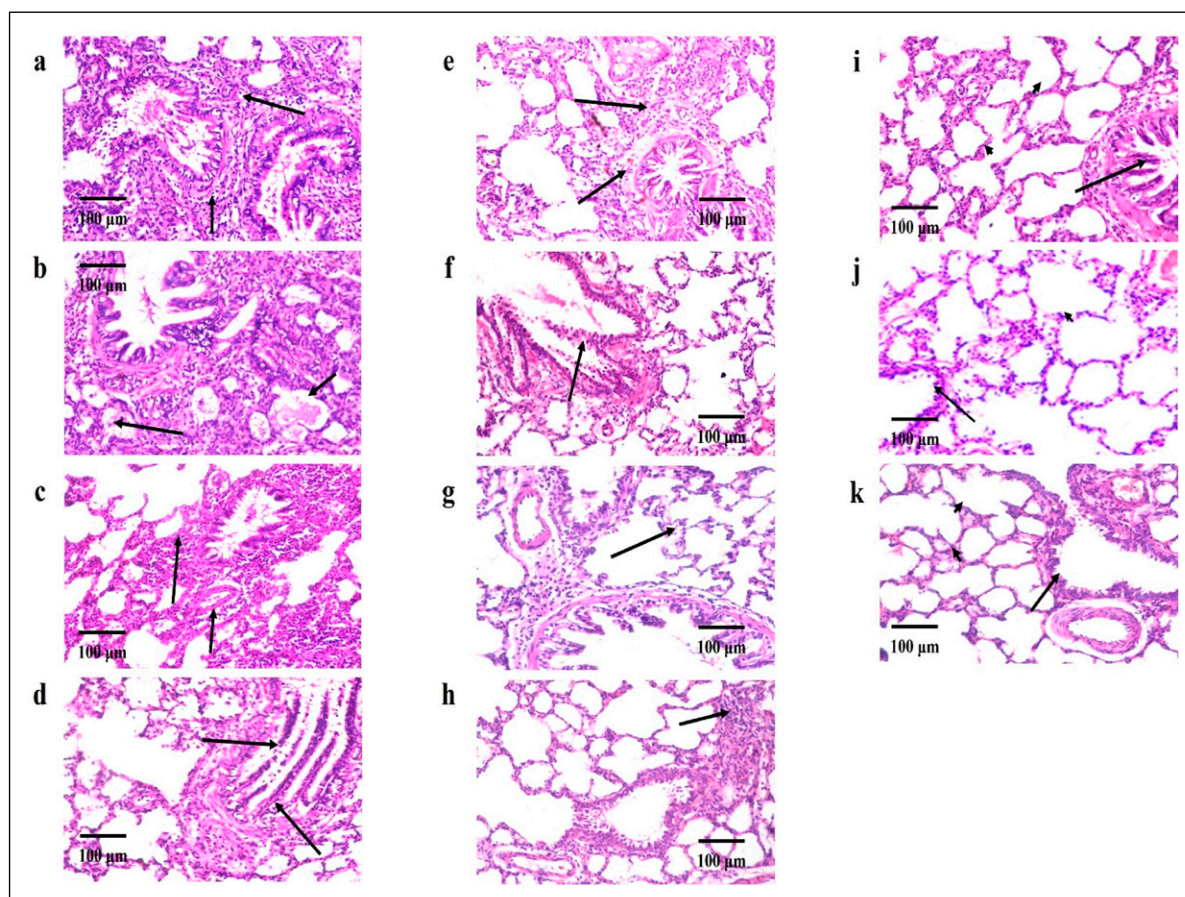


**Figure 5.** Representative lung pathological graphs (H&E X200). (A) massive inflammatory cells infiltration of interstitium tissue (B) Multifocal collapsed area with alveolar oedema. (C) moderate cellular infiltration of the interstitium in peribronchial and perivascular spaces. (D) mild thickening of the inter-alveolar septa and hyperplasia of bronchial epithelial lining. (E) Cellular infiltration in peribronchial and perivascular spaces. (F) Hyperplasia of bronchial epithelial lining with complete loss of bronchial goblet cells. (G) Mild thickening of the inter-alveolar septa. (H) few numbers of cellular aggregation in the interstitium. (I, J, K) normal architecture of alveoli interstitium (**arrow head**) and bronchiolar epithelial lining (**arrow**).

(oxygen saturation and temperature), and markers of inflammation in patients with lung issues. The protective and repairing effect of this combination (MP + R) was found to be more effective than MP or R alone against the lung injury caused by PQ exposure.

When lungs are subjected to detrimental agents, the endothelial cells (EC) and the macrophages become activated following exposure to proinflammatory cytokines such as tumor necrosis factor- $\alpha$  (TNF- $\alpha$ ) and interleukin-1 $\beta$  (IL-1 $\beta$ ). The activated endothelium has an obvious role in inflammation by facilitating the adhesion and migration of polymorphonuclear leukocytes (PMNs) across the endothelial barrier to reach the site of inflammation. Activation and migration of PMNs leads to PMN alveolitis and the damage of vascular endothelial and alveolar epithelial barriers. Intravascular coagulation occurs when the endothelium undergoes a transformation that makes it more likely to promote blood clot formation and the endothelial and epithelial barriers disruption. Pulmonary edema occurs as a consequence of the leakage of plasma and inflammatory cells, causing a surface area reduction of the alveoli and a disruption in

the exchange of gases. Importantly, all the participating proteins in the PMN-EC adhesion are regulated by the NF- $\kappa$ B.<sup>44</sup> The severity and fatality of ALI/ARDS is mainly linked to a “cytokine storm” mediated by NF- $\kappa$ B. This storm is characterized by a significant influx of PMNs and the subsequent release of cytokines, leading to fast deterioration caused by widespread inflammation and coagulation. The canonical NF- $\kappa$ B pathway is triggered by proinflammatory stimuli, including IL-1 $\beta$  and TNF- $\alpha$ .<sup>44</sup> Based on the significantly elevated levels of IL-1 $\beta$ , TNF- $\alpha$ , and NF- $\kappa$ B in the current study, it can be said that PQ intoxication also activated the canonical NF- $\kappa$ B pathway, causing lung tissue injury. In this direction, recently a few publications appeared suggesting that the inhibition of the NF- $\kappa$ B pathway is a new idea to treat PQ-induced lung injury.<sup>45,46</sup> While TNF- $\alpha$  by itself may not cause significant damage, it has the potential to amplify the detrimental effects of IL-1 $\beta$ , NF- $\kappa$ B, and IL-6 in lung inflammation. In our present research, we detected that misoprostol inhibited the inflammatory response and the evolution of ALI through the significant lowering of TNF- $\alpha$ , IL-1 $\beta$ , IL-6, NF- $\kappa$ B, and LPA levels. Administering low-dose radiation decreased the



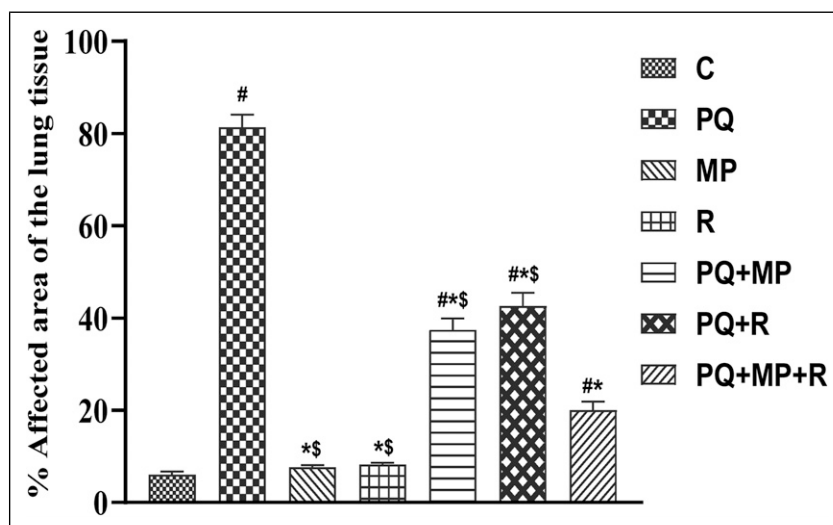


**Figure 6.** Statistical analysis of lung injury score. Data are expressed as mean  $\pm$  S.E. <sup>#</sup> $P \leq 0.05$  vs control. <sup>\*</sup> $P \leq 0.05$  vs PQ-treated group of rats. <sup>\$</sup> $P \leq 0.05$  vs (PQ + MP + R).

inflammatory cytokine levels (TNF- $\alpha$ , IL-1 $\beta$ , and IL-6) in rats intoxicated with paraquat. This was in accord with previous findings indicating the role of R in inflammation inhibition.<sup>47</sup> Within this research, MP and/or R have been investigated for their possible pulmonary protective impact and their therapeutic applications in illnesses resulting from aberrant oxidative stress and inflammation.

Endothelin-1 is a potent vasoconstrictor peptide expressed by different cell types in the lungs, including EC, smooth muscle cells, Clara cells, neuroendocrine cells, and alveolar macrophages<sup>48</sup>; and degraded principally in the pulmonary vasculature. It has been linked to the ALI development, and its levels are higher in ARDS due to both increased production and reduced elimination.<sup>49</sup> It is also one of the growth factors that are possibly to be involved in the EMT, where it is up-regulated by some factors like angiotensin II, thrombin, lipopolysaccharide, TGF- $\beta$ , and epithelial growth factor and downregulated by nitric oxide and prostaglandin.<sup>48</sup>

Both ET-1 and TGF- $\beta$  independently trigger resistance of fibroblasts to apoptosis through signaling pathways involving p38 mitogen-activated protein kinase (MAPK) and pro-survival phosphatidylinositol 3'-OH kinase (PI3K)/AKT.<sup>50</sup> Importantly, it was observed that the rise in ET-1 levels came before the collagen deposition enhancement.<sup>48</sup> ET-1 appears to be functional via the upregulation of TGF- $\beta$ , causing a loss of pro-surfactant protein B and the gain of  $\alpha$ -SMA.<sup>51</sup> Our study detected that ET-1 expression levels in the lung tissue were significantly increased in PQ-injected rats compared to those in the control group. Therefore, it can be suggested that the ET-1 pathway is a possible route for ALI induction by PQ. Some previous studies have indicated that PQ exposure significantly raises the vasoconstrictor factor ET-1 expression degree.<sup>52,53</sup>

The lysophosphatidic acid (LPA) cascade has gained significant attention due to its potential as a valuable biomarker

for understanding the development of many lung disorders and its possible application in therapeutic strategies. The lung tissues contain glycerophospholipids, specifically phosphatidylcholine and phosphatidylethanolamine. These glycerophospholipids are transformed into lysophosphatidylcholine by the enzyme phospholipase A2. Subsequently, lysophosphatidylcholine is changed into LPA by the enzymes lysophospholipase D and autotaxin.<sup>54</sup> It has been reported that ATX, LPA, and their receptors are involved in the EMT-stimulating and the formation of profibrotic cytokines (IL-6, CTGF, and TGF- $\beta$ ) from monocytes and macrophages.<sup>55</sup> Our outcomes declared that in comparison to the control group, PQ significantly increased concentrations of LPA and IL-6. Misoprostol treatment effectively downregulates the elevated expression levels of ET-1 & LPA. The mechanism of low-dose radiation for lowering ET-1 & LPA in paraquat-intoxicated rats may be through multiple routes, including lowering pro-inflammatory cytokines while suppressing the interaction between PMNs and the vascular endothelium and enhancing the polarization of lung macrophages from a pro-inflammatory M-1 phenotype to an anti-inflammatory M-2 phenotype as mentioned previously by Lara et al (2020); Prasanna et al (2020).<sup>56,57</sup> The obtained results clearly reflect the efficacy of MP combined with R against PQ in rats and significantly reversed the ET-1 & LPA high levels caused by PQ.

Peroxisome proliferator-activated receptors (PPAR- $\gamma$ ) are transcription factors that belong to the nuclear receptor superfamily and are activated by ligands. PPAR- $\gamma$ , a member of this superfamily, is present in alveolar epithelial cells, vascular endothelial cells, and macrophages. PPAR- $\gamma$  has a role in the formation of fat cells, sensitivity to insulin, the creation of new mitochondria, reducing inflammation, and protecting the nervous system. Furthermore, PPAR- $\gamma$  has a defensive function in ALI, lung cancer, chronic obstructive pulmonary disease (COPD), and various other pulmonary ailments. Activation of PPAR- $\gamma$  can

decrease the release of inflammatory mediators, but its expression is always suppressed during ALI.<sup>58</sup>

Our results confirmed that PQ poisoning indeed significantly downregulated the expression levels of PPAR- $\gamma$  compared to those that were observed in the control group. Prior administration of MP resulted in a notable rise in PPAR- $\gamma$  activity. These data indicate that the activation of PPAR- $\gamma$  by MP may have an antioxidant effect. In the same concern, PPAR- $\gamma$  upregulation was observed by using low-dose radiation after PQ injection, leading to a decline in the release of inflammatory mediators.<sup>59</sup> This might be due to the suppression of PPAR- $\gamma$  by R, which triggered the DNA binding and transactivation of PPAR- $\gamma$  and raised the transcription of PPAR- $\gamma$  target genes.<sup>60</sup> Our outcomes demonstrated that the concurrent administration of MP in the presence of R ameliorates lung injury induced by paraquat.

In the current study, the histopathological examination in the PQ-intoxicated group was consistent with all the preceding findings where PQ was observed to induce the migration of inflammatory cells into the interstitial and alveolar spaces, as well as enhance the secretion of pro-inflammatory mediators (IL-6, TNF- $\alpha$ , and IL-1 $\beta$ ). Additionally, PQ caused damage to the alveolar epithelial cells, resulting in hemorrhage, edema, and the infiltration of inflammatory cells into the lung tissue. The results of our study, combined with prior reports, indicate that administering early treatment for MP and/or R following PQ injection can prevent lung harm and restore the cellular architecture to its normal state. These findings are corroborated by other investigations in which the lung tissue capillaries dilated and became congested due to a considerable increase in neutrophils. In addition, there was thickening of the lung septa, which did not exhibit any signs of improvement, and the lung injury score was significantly elevated.<sup>61</sup>

In summary, our findings indicate that low-dose gamma radiation and/or misoprostol can be incorporated into a regimen that effectively reduces the severity of paraquat-induced lung injury, as assessed by histological and other investigations. This may be achieved by restricting the hypothesized pathways leading to lung injury. These results broaden the scope of the present therapy and offer a fresh approach to treating and avoiding lung tissue damage. This limited study does not ascertain the applicability of this conclusion to various clinical settings.

## Acknowledgements

Authors owe a tremendous debt of gratitude to Prof. Dr Ahmed Osman of Egypt's Faculty of Veterinary Medicine and the Pathology Department at Cairo University for his invaluable assistance in analyzing lung sections for this work.

## Authors' Contributions

Data collection: Ahmed H. Youssef; experimental design: Shereen M. Galal; analysis and interpretation of the data: Ahmed H. Youssef and Shereen M. Galal; writing manuscript: Ahmed H. Youssef;

overall supervision: Heba H. Mansour, Wafaa Gh. Shousha, Shereen M. Galal and Sara M. Abdo. After reviewing the final manuscript, all authors gave their approval.

## Declaration of Conflicting Interests

The author(s) declared no potential conflicts of interest with respect to the research, authorship, and/or publication of this article.

## Funding

The author(s) received no financial support for the research, authorship, and/or publication of this article.

## Ethical Statement

### Ethical Approval

All experiments followed the 3 Rs principles for animal experimentation (Replace, Reduce, Refine) and were performed according to the CIOMS and ICLAS International Guiding Principles for Biomedical Research Involving animals 2012, approved by the Research Ethics Committee at NCRRT. The approval number is 53 A/23 that dated on December 28, 2023.

### Consent for Publication

The work titled "Unprecedented approach for using misoprostol alongside low-dose gamma radiation to alleviate paraquat-Induced pulmonary injury in rats" has been authored entirely by the individuals mentioned above. No other publisher has published this work or any of its portions, and it won't be submitted anywhere else until the Journal's editing process is finished.

## ORCID iDs

Ahmed H. Youssef  <https://orcid.org/0000-0002-4747-425X>

Heba H. Mansour  <https://orcid.org/0000-0002-6417-7468>

## References

1. Zhang H, Chen S, Zeng M, et al. Apelin-13 administration protects against LPS-induced acute lung injury by inhibiting NF- $\kappa$ B pathway and NLRP3 inflammasome activation. *Cell Physiol Biochem*. 2018;49(5):1918-1932. doi:10.1159/000493653
2. Chen T, Zhu G, Meng X, Zhang X. Recent developments of small molecules with anti-inflammatory activities for the treatment of acute lung injury. *Eur J Med Chem*. 2020;207:112660. doi:10.1016/j.ejmech.2020.112660
3. He YQ, Zhou CC, Yu LY, et al. Natural product derived phytochemicals in managing acute lung injury by multiple mechanisms. *Pharmacol Res*. 2021;163:105224. doi:10.1016/j.phrs.2020.105224
4. Meyer NJ, Gattinoni L, Calfee CS. Acute respiratory distress syndrome. *Lancet*. 2021;398(10300):622-637. doi:10.1016/S0140-6736(21)00439-6
5. Mulugeta S, Nureki S, Beers MF. Lost after translation: insights from pulmonary surfactant for understanding the role of alveolar epithelial dysfunction and cellular quality control in fibrotic lung

- disease. *Am J Physiol Lung Cell Mol Physiol*. 2015;309(6): L507-L525. doi:[10.1152/ajplung.00139.2015](https://doi.org/10.1152/ajplung.00139.2015)
6. Zebialowicz Ahlström J, Massaro F, Mikolka P, et al. Synthetic surfactant with a recombinant surfactant protein C analogue improves lung function and attenuates inflammation in a model of acute respiratory distress syndrome in adult rabbits. *Respir Res*. 2019;20(1):245. doi:[10.1186/s12931-019-1220-x](https://doi.org/10.1186/s12931-019-1220-x)
7. Gouda MM, Shaikh SB, Bhandary YP. Inflammatory and fibrinolytic system in acute respiratory distress syndrome. *Lung*. 2018;196(5):609-616. doi:[10.1007/s00408-018-0150-6](https://doi.org/10.1007/s00408-018-0150-6)
8. Zarilli G, Angerilli V, Businello G, et al. The immunopathological and histological landscape of COVID-19-mediated lung injury. *Int J Mol Sci*. 2021;22(2):974. doi:[10.3390/ijms22020974](https://doi.org/10.3390/ijms22020974)
9. Bochaton-Piallat ML, Gabbiani G, Hinz B. The myofibroblast in wound healing and fibrosis: answered and unanswered questions. *F1000Res*. 2016;5:F1000. doi:[10.12688/f1000research.8190.1](https://doi.org/10.12688/f1000research.8190.1)
10. Upagupta C, Shimbori C, Alsalmi R, Kolb M. Matrix abnormalities in pulmonary fibrosis. *Eur Respir Rev*. 2018;27(148): 180033. doi:[10.1183/16000617.0033-2018](https://doi.org/10.1183/16000617.0033-2018)
11. Savin IA, Zenkova MA, Sen'kova AV. Pulmonary fibrosis as a result of acute lung inflammation: molecular mechanisms, relevant in vivo models, prognostic and therapeutic approaches. *Int J Mol Sci*. 2022;23(23):14959. doi:[10.3390/ijms232314959](https://doi.org/10.3390/ijms232314959)
12. Chen J, Su Y, Lin F, et al. Effect of paraquat on cytotoxicity involved in oxidative stress and inflammatory reaction: a review of mechanisms and ecological implications. *Ecotoxicol Environ Saf*. 2021;224:112711. doi:[10.1016/j.ecoenv.2021.112711](https://doi.org/10.1016/j.ecoenv.2021.112711)
13. Williams JH, Whitehead Z, Van Wilpe E. Paraquat intoxication and associated pathological findings in three dogs in South Africa. *J S Afr Vet Assoc*. 2016;87(1):e1-e9. doi:[10.4102/jsava.v87i1.1352](https://doi.org/10.4102/jsava.v87i1.1352)
14. Palipoch S, Punsawad C, Koomhin P, et al. Aqueous Thunbergia Laurifolia leaf extract alleviates paraquat-induced lung injury in rats by inhibiting oxidative stress and inflammation. *BMC Complement Med Ther*. 2022;22(1):83. doi:[10.1186/s12906-022-03567-4](https://doi.org/10.1186/s12906-022-03567-4)
15. Hathaichoti S, Visitnonthachai D, Ngamsiri P, et al. Paraquat induces extrinsic pathway of apoptosis in A549 cells by induction of DR5 and repression of anti-apoptotic proteins, DDX3 and GSK3 expression. *Toxicol Vitro*. 2017;42:123-129. doi:[10.1016/j.tiv.2017.04.016](https://doi.org/10.1016/j.tiv.2017.04.016)
16. Hu X, Shen H, Wang Y, Zhao M. Liver X receptor agonist TO901317 attenuates paraquat-induced acute lung injury through inhibition of NF- $\kappa$ B and JNK/p38 MAPK signal pathways. *BioMed Res Int*. 2017;2017:4652695. doi:[10.1155/2017/4652695](https://doi.org/10.1155/2017/4652695)
17. Willis BC, Liebler JM, Luby-Phelps K, et al. Induction of epithelial-mesenchymal transition in alveolar epithelial cells by transforming growth factor-beta1: potential role in idiopathic pulmonary fibrosis. *Am J Pathol*. 2005;166(5):1321-1332. doi:[10.1016/s0002-9440\(10\)62351-6](https://doi.org/10.1016/s0002-9440(10)62351-6)
18. Hua XF, Li XH, Li MM, et al. Doxycycline attenuates paraquat-induced pulmonary fibrosis by downregulating the TGF- $\beta$  signaling pathway. *J Thorac Dis*. 2017;9(11):4376-4386. doi:[10.21037/jtd.2017.10.42](https://doi.org/10.21037/jtd.2017.10.42)
19. Gawarammana IB, Buckley NA. Medical management of paraquat ingestion. *Br J Clin Pharmacol*. 2011;72(5):745-757. doi:[10.1111/j.1365-2125.2011.04026.x](https://doi.org/10.1111/j.1365-2125.2011.04026.x)
20. Barberà JA, Román A, Gómez-Sánchez M, et al. Guidelines on the diagnosis and treatment of pulmonary hypertension: summary of recommendations. *Arch Bronconeumol*. 2018;54(4): 205-215. doi:[10.1016/j.arbres.2017.11.014](https://doi.org/10.1016/j.arbres.2017.11.014)
21. Li P, Gu L, Tan J, et al. A randomised controlled trial on roles of prostaglandin E1 nebulization among patients undergoing one lung ventilation. *BMC Pulm Med*. 2022;22(1):37. doi:[10.1186/s12890-022-01831-4](https://doi.org/10.1186/s12890-022-01831-4)
22. Gobejishvili L, Ghare S, Khan R, et al. Misoprostol modulates cytokine expression through a cAMP pathway: potential therapeutic implication for liver disease. *Clin Immunol*. 2015; 161(2):291-299. doi:[10.1016/j.clim.2015.09.008](https://doi.org/10.1016/j.clim.2015.09.008)
23. Mehta P, McAuley DF, Brown M, et al. COVID-19: consider cytokine storm syndromes and immunosuppression. *Lancet*. 2020; 395(10229):1033-1034. doi:[10.1016/s0140-6736\(20\)30628-0](https://doi.org/10.1016/s0140-6736(20)30628-0)
24. Wilson GD, Mehta MP, Welsh JS, Chakravarti A, Rogers CL, Fontanesi J. Investigating low-dose thoracic radiation as a treatment for COVID-19 patients to prevent respiratory failure. *Radiat Res*. 2020;194(1):1-8. doi:[10.1667/rade-20-00108.1](https://doi.org/10.1667/rade-20-00108.1)
25. Dhawan G, Kapoor R, Dhawan R, et al. Low dose radiation therapy as a potential life saving treatment for COVID-19-induced acute respiratory distress syndrome (ARDS). *Radiother Oncol*. 2020;147:212-216. doi:[10.1016/j.radonc.2020.05.002](https://doi.org/10.1016/j.radonc.2020.05.002)
26. Kirkby C, Mackenzie M. Is low dose radiation therapy a potential treatment for COVID-19 pneumonia? *Radiother Oncol*. 2020;147:221. doi:[10.1016/j.radonc.2020.04.004](https://doi.org/10.1016/j.radonc.2020.04.004)
27. Pourgholamhossein F, Sharififar F, Rasooli R, et al. Thymoquinone effectively alleviates lung fibrosis induced by paraquat herbicide through down-regulation of pro-fibrotic genes and inhibition of oxidative stress. *Environ Toxicol Pharmacol*. 2016; 45:340-345. doi:[10.1016/j.etap.2016.06.019](https://doi.org/10.1016/j.etap.2016.06.019)
28. Nasr AY. Morphological, biochemical, histological, and ultrastructural protective effects of misoprostol on cisplatin induced-hepatotoxicity in adult male rats. *Saudi Med J*. 2013;34(12): 1237-1247.
29. Al-Massarani G, Almohamad K. Evaluation of circulating endothelial cells in the rat after acute and fractionated whole-body gamma irradiation. *Nukleonika*. 2014;59(4):145-151. doi:[10.2478/nuka-2014-0021](https://doi.org/10.2478/nuka-2014-0021)
30. Bancroft JD, Gamble M. *Theory and Practice of Histological Techniques*. 6th ed. Journal of Neuropathology & Experimental Neurology: Oxford Academic; 2008.
31. Eldh T, Heinzelmann F, Velalakan A, Budach W, Belka C, Jendrossek V. Radiation-induced changes in breathing frequency and lung histology of C57BL/6J mice are time- and dose-dependent. *Strahlenther Onkol*. 2012;188(3):274-281. doi:[10.1007/s00066-011-0046-3](https://doi.org/10.1007/s00066-011-0046-3)
32. Yang J, Li S, Wang L, et al. Ginsenoside Rg3 attenuates lipopolysaccharide-induced acute lung injury via MerTK-dependent activation of the PI3K/AKT/mTOR pathway. *Front Pharmacol*. 2018;9:850. doi:[10.3389/fphar.2018.00850](https://doi.org/10.3389/fphar.2018.00850)

33. Meng XM, Nikolic-Paterson DJ, Lan HY. TGF- $\beta$ : the master regulator of fibrosis. *Nat Rev Nephrol*. 2016;12(6):325-338. doi:10.1038/nrneph.2016.48
34. Cheresh P, Kim SJ, Tulasiram S, Kamp DW. Oxidative stress and pulmonary fibrosis. *Biochim Biophys Acta*. 2013;1832(7):1028-1040. doi:10.1016/j.bbdis.2012.11.021
35. Blank U, Karlsson S. The role of Smad signaling in hematopoiesis and translational hematology. *Leukemia*. 2011;25(9):1379-1388. doi:10.1038/leu.2011.95
36. Chen QK, Lee K, Radisky DC, Nelson CM. Extracellular matrix proteins regulate epithelial-mesenchymal transition in mammary epithelial cells. *Differentiation*. 2013;86(3):126-132. doi:10.1016/j.diff.2013.03.003
37. Kono M, Nakamura Y, Suda T, et al. Plasma CCN2 (connective tissue growth factor; CTGF) is a potential biomarker in idiopathic pulmonary fibrosis (IPF). *Clin Chim Acta*. 2011;412(23-24):2211-2215. doi:10.1016/j.cca.2011.08.008
38. Ren Y, Jian X, Zhang Z, Ning Q, Kan B, Kong L. Effects of tacrolimus on the TGF- $\beta$ /SMAD signaling pathway in paraquat-exposed rat alveolar type II epithelial cells. *Mol Med Rep*. 2020;22(5):3687-3694. doi:10.3892/mmr.2020.11453
39. Rodríguez-Tomás E, Acosta JC, Torres-Royo L, et al. Effect of low-dose radiotherapy on the circulating levels of paraoxonase-1-related variables and markers of inflammation in patients with COVID-19 pneumonia. *Antioxidants*. 2022;11(6):1184. doi:10.3390/antiox11061184
40. Chen H, Liu X, Su Y, et al. Notch signaling pathway mediates the immunomodulatory mechanism of Yangfei Huoxue decoction alleviating bleomycin-induced pulmonary fibrosis in rats. *J Tradit Chin Med*. 2020;40(2):204-211.
41. Wynn TA. Integrating mechanisms of pulmonary fibrosis. *J Exp Med*. 2011;208(7):1339-1350. doi:10.1084/jem.20110551
42. Li Y, Lian Z, Li Q, et al. Molecular mechanism by which the Notch signaling pathway regulates autophagy in a rat model of pulmonary fibrosis in pigeon breeder's lung. *Open Med*. 2023;18(1):20230629. doi:10.1515/med-2023-0629
43. Arenas M, Algara M, De Febrer G, et al. Could pulmonary low-dose radiation therapy be an alternative treatment for patients with COVID-19 pneumonia? Preliminary results of a multicenter SEOR-GICOR nonrandomized prospective trial (IPA-COVID trial). *Strahlenther Onkol*. 2021;197(11):1010-1020. doi:10.1007/s00066-021-01803-3
44. Millar MW, Fazal F, Rahman A. Therapeutic targeting of NF- $\kappa$ B in acute lung injury: a double-edged sword. *Cells*. 2022;11(20):3317. doi:10.3390/cells11203317
45. Jin H. Imrecoxib inhibits paraquat-induced pulmonary fibrosis through the NF- $\kappa$ B/Snail signaling pathway. *Comput Math Methods Med*. 2020;2020:6374014. doi:10.1155/2020/6374014
46. Sun H, Jiang Y, Song Y, et al. The MUC5B mucin is involved in paraquat-induced lung inflammation. *Oxid Med Cell Longev*. 2020;2020:7028947. doi:10.1155/2020/7028947
47. Kim JY, Lee YR, Lee YA, et al. Preventive and therapeutic effects of low-dose whole-body irradiation on collagen-induced rheumatoid arthritis in mice. *J Radiat Res*. 2024;65(2):177-186. doi:10.1093/jrr/rrad101
48. Fonseca C, Abraham D, Renzoni EA. Endothelin in pulmonary fibrosis. *Am J Respir Cell Mol Biol*. 2011;44(1):1-10. doi:10.1165/rcmb.2009-0388TR
49. Vassiliou AG, Kotanidou A, Dimopoulou I, Orfanos SE. Endothelial damage in acute respiratory distress syndrome. *Int J Mol Sci*. 2020;21(22):8793. doi:10.3390/ijms21228793
50. Kulasekaran P, Scavone CA, Rogers DS, Arenberg DA, Thannickal VJ, Horowitz JC. Endothelin-1 and transforming growth factor-beta1 independently induce fibroblast resistance to apoptosis via AKT activation. *Am J Respir Cell Mol Biol*. 2009;41(4):484-493. doi:10.1165/rcmb.2008-0447OC
51. Yamada M, Kuwano K, Maeyama T, et al. Dual-immunohistochemistry provides little evidence for epithelial-mesenchymal transition in pulmonary fibrosis. *Histochem Cell Biol*. 2008;129(4):453-462. doi:10.1007/s00418-008-0388-9
52. Fan L, Xu J, Lv T, Lu M. Asthma attacks: patients who survived paraquat poisoning. *J Toxicol Sci*. 2022;47(4):147-149. doi:10.2131/jts.47.147
53. Pang L, Deng P, Liang YD, et al. Lipoic acid antagonizes paraquat-induced vascular endothelial dysfunction by suppressing mitochondrial reactive oxidative stress. *Toxicol Res*. 2019;8(6):918-927. doi:10.1039/c9tx00186g
54. Law SH, Chan ML, Marathe GK, Parveen F, Chen CH, Ke LY. An updated review of lysophosphatidylcholine metabolism in human diseases. *Int J Mol Sci*. 2019;20(5):1149. doi:10.3390/ijms20051149
55. Richeldi L, Fernández Pérez ER, Costabel U, et al. Pamrevlumab, an anti-connective tissue growth factor therapy, for idiopathic pulmonary fibrosis (PRAISE): a phase 2, randomised, double-blind, placebo-controlled trial. *Lancet Respir Med*. 2020;8(1):25-33. doi:10.1016/s2213-2600(19)30262-0
56. Lara PC, Burgos J, Macias D. Low dose lung radiotherapy for COVID-19 pneumonia. The rationale for a cost-effective anti-inflammatory treatment. *Clin Transl Radiat Oncol*. 2020;23:27-29. doi:10.1016/j.ctro.2020.04.006
57. Prasanna PG, Woloschak GE, DiCarlo AL, et al. Low-dose radiation therapy (LDRT) for COVID-19: benefits or risks? *Radiat Res*. 2020;194(5):452-464. doi:10.1667/rade-20-00211.1
58. Tang Y, Wei K, Liu L, Ma J, Wu S, Tang W. Activation of PPAR $\gamma$  protects obese mice from acute lung injury by inhibiting endoplasmic reticulum stress and promoting mitochondrial biogenesis. *PPAR Res*. 2022;2022:7888937. doi:10.1155/2022/7888937
59. Korbecki J, Bobiński R, Dutka M. Self-regulation of the inflammatory response by peroxisome proliferator-activated receptors. *Inflamm Res*. 2019;68(6):443-458. doi:10.1007/s00011-019-01231-1
60. Chatterjee P, Choudhary GS, Sharma A, et al. PARP inhibition sensitizes to low dose-rate radiation TMPRSS2-ERG fusion gene-expressing and PTEN-deficient prostate cancer cells. *PLoS One*. 2013;8(4):e60408. doi:10.1371/journal.pone.0060408
61. Zhang Z, Nian Q, Chen G, Cui S, Han Y, Zhang J. Klotho alleviates lung injury caused by paraquat via suppressing ROS/P38 MAPK-regulated inflammatory responses and apoptosis. *Oxid Med Cell Longev*. 2020;2020:1854206. doi:10.1155/2020/1854206